Finite length and solvent analysis effects on the squash mode of single walled carbon nanotubes

ARTICLE *in* APPLIED PHYSICS LETTERS · OCTOBER 2013

Impact Factor: 3.3 · DOI: 10.1063/1.4824849

3 AUTHORS, INCLUDING:

Nick Quirke
Imperial College London
146 PUBLICATIONS **6,108** CITATIONS
SEE PROFILE

Dominic Zerulla
University College Dublin
59 PUBLICATIONS **328** CITATIONS
SEE PROFILE

Finite Length and Solvent Analysis Effects on the Squash Mode of Single Walled Carbon Nanotubes.

C. de Fréin,[1] N. Quirke,[2, a)] and D. Zerulla[1, b)]
[1)] *Plasmonic and Ultra-fast Nanooptics, School of Physics, University College Dublin, Belfield, Dublin 4, Ireland*
[2)] *Department of Chemistry, Imperial College, London, UK*

(Dated: September 23, 2013)

Nanotube diameters (d) are usually characterized using the radial breathing mode d^{-1}, the squash mode frequency (f) however is predicted to vary as d^{-2}. We demonstrate using the MM+ forcefield that for lengths < 9 nm the symmetric (SSM) and asymmetric (ASM) squash modes ((10,0) SWNT) are non-degenerate with $\Delta f \leq 55$ cm^{-1}. In solution, the SWNT-water interaction upshifts the ASM by 20 cm^{-1} and the SSM by 10 cm^{-1}. Such asymmetries could be used to simultaneously characterize the length and diameter of short nanotubes for applications including nanoresonators and biomedical probes.

PACS numbers: 62.25.+g, 62.10.+s
Keywords: Raman Spectroscopy, Carbon Nanotubes, Radial Modes.

Since their discovery in 1991 by Iijima[1], the properties and potential applications of Single Wall Carbon Nanotubes (SWNTs) have been the object of extensive research[2]. Many well-known properties, such as mechanical and electrical properties, are dictated by the chirality of the nanotube: zigzag (n,0), armchair (n,n) and chiral (n,m)[3]. Raman Spectroscopy, implemented to obtain vibrational spectra, is one of the most powerful tools used to characterise SWNTs. It offers a unique method for identifying SWNTs in a given sample.

Group theory predicts up to 16 Raman-active modes at k = 0 for all nanotubes (Saito *et. al.* 1998)[4]. Experimentally, the Raman spectra are dominated by the radial breathing mode (RBM), the D mode and the G mode. The RBM is typically used to determine the diameter range of SWNTs in a sample, the D mode can be used to establish the structural quality of the SWNTs and the shape of the G mode can be used to determine the conductivity of the SWNTs. However, there is yet another potentially important Raman-active mode that is radially dependent, the squash mode (SM), also known as the low frequency E_{2g} mode[4] in terms of group theory. The removal of the doubly degenerate nature of the SM for short tube lengths, which is yet to be found experimentally, is demonstrated in this paper. The vibrational motion of both SM degeneracies and the RBM is depicted in figure 1. The lower frequency symmetric squash mode (SSM) can be visualised as radial displacements along the full length of the SWNT along one a axis which is perpendicular to the SWNT axis (along the length of the SWNT). The higher frequency asymmetric squash mode (ASM), consists of perpendicular radial displacements at opposite ends of the SWNT.

Radial modes of SWNTs, such as the RBM and the SM, are significant as they can offer a means to identifying and distinguishing SWNTs in a sample based on their diameter. It is well known that the lineshape of the RBM is strongly influenced by resonance effects, therefore not all SWNTs in a given sample can be identified with a particular excitation[5]. But the ability to identify the SM experimentally would lead to further radial characterisation of the SWNTs in a sample containing many chiralities. In such a sample, it is also important to understand the effect of finite length on the frequency of these radial modes. It is also important to understand environmental effects, such as SWNT-solvent interactions, on the frequency of the radial modes, if SWNTs are to be used in medical treatments[6,7]. Length dependence studies are necessary if a SWNT is to be used as a nanomechanical resonator, one needs to know not only the lowest natural frequency but also the corresponding mode shape for proper tuning[8].

A variety of theoretical methods have been used to characterise the SM. Initial work by Saito *et. al.*[4], used zone-folding and force-constant models to show that the lowest phonon mode with non-zero energy at k=0 is the SM. They found that the frequency of the SM for a (10,10) nanotube was extremely low, 17 cm^{-1}. Bond polarization theory predicts that the SM lies in the range of 18 - 34 cm^{-1} for armchair nanotubes, n = 8 - 11[9]. Tight binding analysis performed for a range of armchair and zigzag SWNTs, showed that there was a significant upshift in the frequency of the SM when the isolated SWNT was placed in a bundle[10]. The spectral moments method in the framework of the bond-polarisation theory showed that the SM frequency length dependence was only apparent for SWNTs <30 nm[11]. The elastic continuum model performed on armchair SWNTs found that the SM was radially dependent, but became independent of length at L/d = 2.0[12]. Research by Gupta *et. al.*[8], implementing the MM3 forcefield, refer to the Asymmetric SM (ASM) and the Symmetric SM (SSM) as the Rayleigh and Love modes respectively. For a (20,0) SWNT, with

[a)] Authors to whom correspondence should be addressed. Electronic mail:n.quirke@imperial.ac.uk
[b)] Electronic mail:dominic.zerulla@ucd.ie

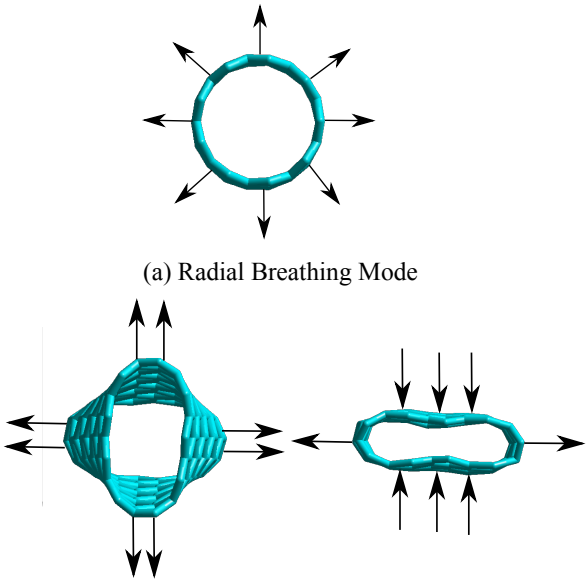

Figure 1. Low Frequency Vibrational Modes of SWNTs. All modes are exaggerated for clarity.

aspect ratio 4.58, the Rayleigh mode was 18.95 cm^{-1} and the Love mode was 19.12 cm^{-1}. Extensive simulations using DFT at the B3LYP/6-31G level performed by Aydin *et. al.* found a power law described the dependence of the SM on diameter[13]. Analysis by Chomdhury *et. al.* using UFF force field for armchair and zigzag SWNTs, found that the natural frequencies are inversely proportional with the aspect ratio and that the SM is independent of chirality[14].

Here, MM+ was performed to investigate the low frequency vibrations of SWNTs. The MM+ force field designed to calculate the interaction between aromatic molecules[15], has been used to investigate the interaction between a carbon nanotube (CNT) and graphene sheet as a means to describing the contact properties between a CNT atomic force microscopy (AFM) tip and a graphite surface[16]. Palacin *et. al.*[17] used the MM+ force field to support experimental data regarding the rigidity of different types of zinc porphyrin linkers on a SWNT.

The purpose of the research reported in this letter, is to investigate the dependence of the SM frequency on the SWNTs environment and their structure. The radial dependence of the SM frequency is found for a series of zigzag SWNTs and compared with fits from the literature[3,8,10,12]. The length dependence of the SM is calculated for zigzag and chiral SWNTs. Finally, the dependence of the SM on SWNT-water interactions was analysed. A significant upshift of both the SSM and the ASM is found.

Molecular mechanics calculations were performed with HYPERCHEM V.8.0 utilising the MM+ forcefield and using the parameters and atom types of the MM2 functional form[18,19], modified to incorporate nonbonded cutoffs (using switched or shifted smoothed), periodic boundary conditions and the bond stretch term switched from cubic to quadratic form at long ranges. All components of the MM+ force field (bond, angle, torsion, nonbonded, electrostatic, hydrogen-bonded) were included in the calculations.

MM+ does not use a Lennard-Jones potential to describe the van der Waals (vdW) interactions but combines an exponential repulsion with an attractive $\frac{1}{R^6}$ dispersion interaction. The vdW term is calculated as[20]

$$E_{vdW} = \sum \varepsilon_{ij} \left[2.9 \times 10^5 exp(-12.5\rho_{ij}) - 2.25\rho_{ij}^{-6}\right] \quad (1)$$

where $\rho_{ij} = \frac{R_{ij}}{r^*_{ij}}, r^*_{ij} = r^*_i + r^*_j, r^*_i$ is the vdW radius for the atom of type i and R_{ij} is the distance between the core of the two atoms, and $\varepsilon_{ij} = \sqrt{\varepsilon_i \varepsilon_j}$ and the hardness parameters ε_i determine the depth of the attractive well and are defined for a pair of atoms.

The analysis was performed on chiral (n,m) and zigzag (n,0) SWNTs. The structure of the zigzag SWNT was obtained using the buckytube.tcl script[21]. The structures of the chiral SWNTs were generated with NANOTUBE MODELER software[22]. The geometry of the isolated SWNT in a vacuum system was optimised using the Polak-Ribiere conjugate-gradient method applied to the MM+ force field. The optimisation was terminated when the gradient of the molecular coordinates fell below 0.001 kcal/(Åmol). The frequencies of the SM of the SWNTs were obtained using the vibrational and rotational analysis. The normal modes and harmonic frequencies are determined via diagonalization of the Hessian matrix. Density functional theory (DFT) at the B3LYP/6-31G level[13] was used to verify the use of MM+ for these calculations.

Environmental influences on the frequency of the SM were investigated by adding a periodic box of pre-equilibrated TIP3P water (density of water molecules = 0.03 molecules/$Å^3$) to the SWNT system. Geometric optimisation and frequency calculations were performed using the method described above for the isolated SWNT system. The inner and outer radius cutoffs used were 4 and 14 Å respectively. The switching function, switch $(r - r_0, -\frac{1}{3}CS, -\frac{4}{3}CS)CS(r - r_0)$, was used to alleviate the nonphysical behaviours caused by imposing a nonbonded cut-off.

The dependence of the symmetric squash mode (SSM) frequency on the radius of the SWNT was investigated. Calculations were performed on zigzag nanotubes, (n,0), n = 8 - 16. According to Li *et. al.*[12], the frequency of the radial modes becomes independent of length when L/d exceeds $\sim$ 2, that is, when the structure becomes more of a geometric tube than a ring. Therefore, for the purpose of this radial dependence analysis, the length of all zigzag SWNTs investigated was 4.3 nm.

The power law correlation in the form $\omega(r) = ar^b$, is typically used to describe the radial dependence of the frequency of the squash mode[3,13,10,12]. The data shown in figure 2, obtained using the MM+ forcefield, is in

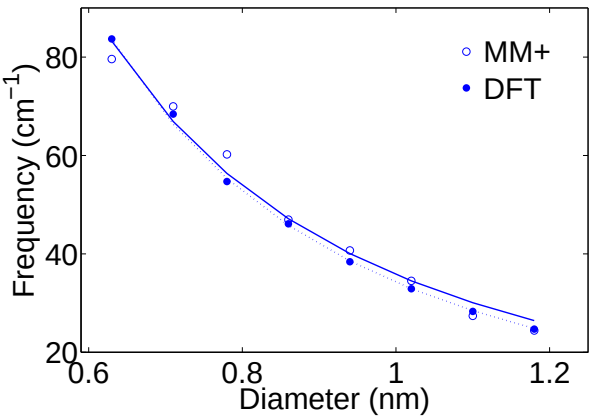

Figure 2. Frequency of the symmetric squash mode as a function of diameter. The solid and dashed lines are fits of the data to power laws for MM+ and DFT respectively, with coefficients reported in the text and listed in table I.

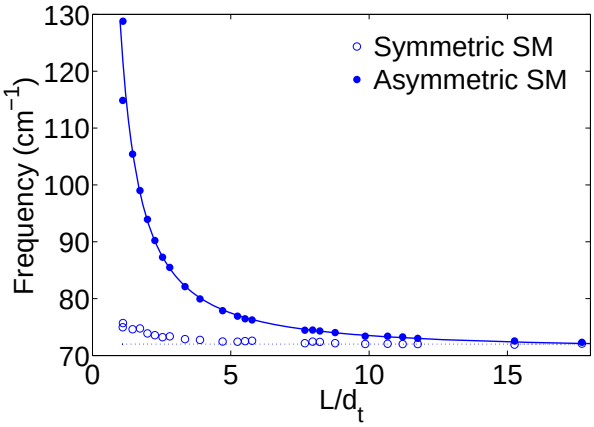

Figure 3. Frequency of the symmetric and asymmetric squash mode as a function of L/d. The solid line is the power law fit for the asymmetric data. The dashed line represents the asymptotic value. Details of all power law fit parameters are reported in the text and listed in table II.

Table I. Comparison between parameter values. [b]Work for this paper.

Method	Exponent
Non-bond Polarization Theory[3]	-1.95 ± 0.03
DFT[13]	-1.935 ± 0.058
MM+ [b]	-1.808 ± 0.271
Tightbinding Method[10]	-1.912 ± 0.04
Elastic Continuum Model[12]	-1.938 ± 0.08

agreement with this expected power law correlation. The MM+ forcefield can also be verified for this diameter range, via comparison with data obtained by using density functional theory (DFT) at the B3LYP/6-31G level[13]. The largest deviation between both methods occurs at smaller diameters ($d_t < 0.63$ nm). It is not surprising that this deviation from the atomistic method occurs most noticeably for smaller diameters which have the smallest number of atoms and the highest curvature. Therefore, only larger diameter ranges were examined.
The extensive work on the radial dependence of the squash mode frequency is documented in table I. The large range of computational methods that have been employed to understand this dependence, including the MM+ force field used in this work, all agree that the dependence is near $1/r^2$.
Both the RBM and the SM are inversely dependent on the radius of the SWNTs. The dependence is linear for the RBM. The radial dependence of the SM can be used as an alternative identification method of SWNTs in bundles. This illustrates the importance of a thorough investigation of the SM.

The frequency of the SM was calculated for zigzag, (10,0), and chiral, (6,5) and (6,3), SWNTs as a function of length. Discrete values for the length ranged from 0.73 nm to 13.80 nm. At $L/d_t < 8$, it was found that the Squash Mode became non-degenerate. Non-resonant bond polarization theory used by Saito *et. al.*[4] confirmed that the E_{2g} becomes doubly degenerate for infinite length tubes. Rahmani *et. al.* found that for all chiralities there is an increase in the number of Raman active modes when the tube length decreases[11]. The splitting of the degeneracy is shown for a (10,0) SWNT in figure 3. Here it is seen that the asymmetric SM (ASM) has significantly higher frequencies at shorter L/d_t than its symmetric SM (SSM) counterpart. In fact, the separation between the modes is as great as 53 cm^{-1} at $L/d_t \simeq 1.1$ for the (10,0) nanotube. This illustrates the extreme sensitivity of the SM to length. A power law $\omega(l) = al^{-b} + c$ was found for both degeneracies. At $L/d_t \simeq 8$, the frequency of the SM only deviates from its asymptotic value by 3%. The length dependence of the SWNTs is shown to be only significant for shorter tubes. Similar trends were found for the chiral SWNTs. These results are summarised in table II. The frequencies of all the Raman modes, including radial breathing mode (RBM) and G band, downshift simultaneously with increasing temperature[23]. For the RBM this amounts to a shift of 1% between an extrapolated 0 K frequency and 300 K[24], therefore a small decrease in the squash mode frequencies of this order at 300 K is expected.

In the following we illustrate the dependence of the frequency of the SM when the SWNTs are surrounded by a solvent. The frequency of the SM was calculated for a chiral (6,3) SWNT immersed in water. Discrete values for the length of the chiral nanotube ranged from 1 - 5 nm. The shorter lengths enabled us to see the effect of the fluid-SWNT interaction on both degeneracies. An upshift in frequency for all lengths and both degeneracies

Table II. Details of coefficients for power law fits for three nanotubes.

Nanotube	Chirality	SSM	ASM
(10,0)	Zigzag	-0.87	-1.35
(6,5)	Chiral	-1.27	-2.24
(6,3)	Chiral	-0.68	-1.95

was found. Figure 4 shows the change in SM frequency for all lengths for both the vacuum and water systems. The power law fits in this figure illustrate that the splitting of the degeneracy is significant for both the solvent and vacuum based systems. Both experimental and computational studies have shown that the frequency of the RBM is upshifted due to fluid-nanotube interactions[25,26]. Longhurst *et. al.*[26] found that van der Waals interactions between the SWNT and the fluid shell induce an upshift in the RBM. Therefore an upshift in the SM, another radial mode, is expected. This upshift is shown by the simulations performed and demonstrated in figure 4. Additionally the average upshift of the ASM was 2.3 times greater than that of the SSM, indicative of the superior sensitivity of the ASM to environmental effects. The maximum upshift calculated for the asymmetric mode was 24 cm^{-1}. As this upshift is four times greater than average values experimentally found by Izard *et. al.*[25] for the RBM, it could lead to more accurate measurements of the upshift of Raman active modes of SWNTs in solution. The tight-binding analysis performed by Kahn *et. al.*[10], showed that the upshift for the SM is high, when the nanotubes are in bundles. In light of the experimental[25] and simulation[26] findings demonstrating the dependence of the RBM frequency on environment, as well as the analysis by Kahn *et. al.*[10] showing the frequency of the SM dependence on bundling, the upshift of the ASM and SSM when the SWNT is surrounded by solvent, evidenced in figure 4, is expected. The superior sensitivity of the ASM, for the finite lengths investigated, is also shown in figure 4.

In conclusion, the vibrational behaviour of the low frequency SM of SWNTs (zigzag and chiral) is reported. The molecular mechanics forcefield MM+ is implemented to analyse the dependence of the SM on structural changes to the SWNT as well as environmental changes. The frequency of the SM is shown to increase with decreasing radius of SWNTs. The double degeneracies of the SM for long SWNTs are removed for L/d < 8. The difference between the ASM and the SSM frequencies at L = 1 nm is 53 cm^{-1} for (10,0). The frequency of the ASM is more sensitive to environmental change than the frequency of the SSM and the frequency of the ASM, for L = 1 - 5 nm, was on average twice that of the SSM when immersed in TIP3P water. In view of the results presented here, it follows that the frequency of the SM depends both on SWNT structure and the environment. Once confirmed experimentally the high sensitivity of the SM frequency could be significant in the design of medical probes and nanomechanical resonators.

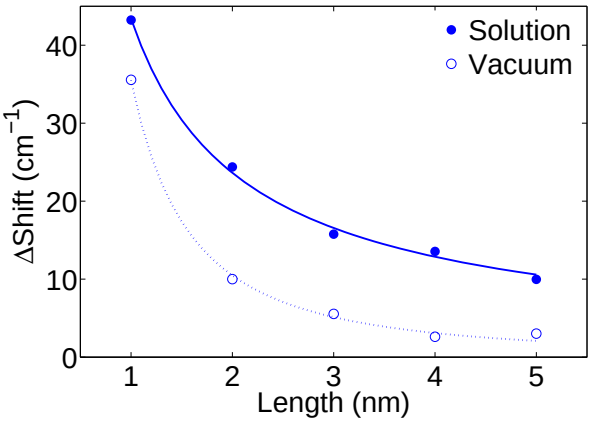

Figure 4. Difference in SM frequency for solution and vacuum systems. The solid circles show the difference between the SSM and ASM frequency in the solution based environment. The empty circles show the difference between the SSM and the ASM in the vacuum environment.

REFERENCES

[1] S. Iijima, "Helical microtubules of graphitic carbon," Nature **354**, 56–58 (1991).

[2] M. Dresselhaus, G. Dresselhaus, R. Saito, and A. Jorio, "Raman spectroscopy of carbon nanotubes," Physics Reports **409**, 47 – 99 (2005).

[3] M. S. Dresselhaus, G. Dresselhaus, J. C. Charlier, and E. Hernandez, "Electronic, thermal and mechanical properties of carbon nanotubes," Philosophical Transactions of The Royal Society A: Mathematical, Physical and Engineering Sciences **362**, 2065–2098 (2004).

[4] R. Saito, T. Takeya, T. Kimura, G. Dresselhaus, and M. S. Dresselhaus, "Raman intensity of single-wall carbon nanotubes," Phys. Rev. B **57**, 4145–4153 (1998).

[5] M. A. Pimenta, A. Marucci, S. D. M. Brown, and M. J. Matthews, "Resonant raman effect in single-wall carbon nanotubes," Journal of Materials Research **13**, 2396–2404 (1998).

[6] D. Pantarotto, J.-P. Briand, M. Prato, and A. Bianco, "Translocation of bioactive peptides across cell membranes by carbon nanotubes," Chem. Commun. **1**, 16–17 (2004).

[7] A. Bianco, K. Kostarelos, and M. Prato, "Applications of carbon nanotubes in drug delivery," Current Opinion in Chemical Biology **9**, 674 – 679 (2005).

[8] S. S. Gupta, F. G. Bosco, and R. C. Batra, "Breakdown of structural models for vibrations of single-wall zigzag carbon nanotubes," Journal of Applied Physics **106**, 063527–1 (2009).

[9] A. M. Rao, E. Richter, S. Bandow, B. Chase, P. C. Eklund, K. A. Williams, S. Fang, K. R. Subbaswamy, M. Menon, A. Thess, R. E. Smalley, G. Dresselhaus, and M. S. Dresselhaus, "Diameter-selective raman scattering from vibrational modes in carbon nanotubes," Science **275**, 187–191 (1997).

[10] D. Kahn and J. P. Lu, "Vibrational modes of carbon nanotubes and nanoropes," Phys. Rev. B **60**, 6535–6540 (1999).

[11] A. Rahmani, J.-L. Sauvajol, S. Rols, and C. Benoit, "Nonresonant raman spectrum in infinite and finite single-wall carbon nanotubes," Phys. Rev. B **66**, 125404 (2002).

[12] G. Li, J. G. A. Lamberton, and J. R. Gladden, "Acoustic modes of finite length homogeneous and layered cylindrical shells: Single

and multiwall carbon nanotubes," Journal of Applied Physics **104**, 033524–033530 (2008).

[13] M. Aydin and D. L. Akins, "Calculated dependence of vibrational band frequencies of single-walled and double-walled carbon nanotubes on diameter," Vibrational Spectroscopy **53**, 163–172 (2010).

[14] R. Chowdhury, S. Adhikari, C. Wang, and F. Scarpa, "A molecular mechanics approach for the vibration of single-walled carbon nanotubes," Computational Materials Science **48**, 730735 (2010).

[15] A. Hocquet and M. Langgard, "An evaluation of the mm+ force field," Molecular modeling annual **4**, 94–112 (1998).

[16] M. Seydou, S. Marsaudon, J. Buchoux, J. P. Aíme, and A. M. Bonnot, "Molecular mechanics investigations of carbon nanotube and graphene sheet interaction," Phys. Rev. B **80**, 245421 (2009).

[17] T. Palacin, H. L. Khanh, B. Jousselme, P. Jegou, A. Filoramo, C. Ehli, D. M. Guldi, and S. Campidelli, "Efficient functionalization of carbon nanotubes with porphyrin dendrons via click chemistry," Journal of the American Chemical Society **131**, 15394–15402 (2009), pMID: 19919163.

[18] N. L. Allinger, "Conformational analysis. 130. MM2. A hydrocarbon force field utilizing V1 and V2 torsional terms," Journal of The American Chemical Society **99**, 8127–8134 (1977).

[19] N. L. Allinger, X. Zhou, and J. Bergsma, "Molecular mechanics parameters," Journal of Molecular Structure: Theochem **312**, 69 – 83 (1994).

[20] *Computational Chemistry, Hyperchem Manual* (Hypercube, Ontario, Canada., 1994).

[21] "Hyperchem v8.0, support package," .

[22] JCristalSoft, "Nanotube modeler, manual," (2005).

[23] P. V. Huong, R. Cavagnat, P. M. Ajayan, and O. Stephan, "Temperature-dependent vibrational spectra of carbon nanotubes." Phys. Rev. B **51**, 10048 (1995).

[24] Z. Zhou, X. Dou, L. Ci, L. Song, D. Liu, Y. Gao, J. Wang, L. Liu, W. Zhou, S. Xie, and D. Wan, "Temperature dependence of the raman spectra of individual carbon nanotubes." J. Phys. Chem. B **110**, 1206–1209 (2006).

[25] N. Izard, D. Riehl, and E. Anglaret, "Exfoliation of single-wall carbon nanotubes in aqueous surfactant suspensions: A raman study," Phys. Rev. B **71**, 195417 (2005).

[26] M. J. Longhurst and N. Quirke, "The environmental effect on the radial breathing mode of carbon nanotubes in water," Journal of Chemical Physics **124**, 234708–234715 (2006).